Photovoltage and J-V features of porous silicon

MC. Arenas*[,a,b], Hailin Hu[a], J. Antonio del Río[a], Oscar H. Salinas[a]
[a]*Centro de Investigación en Energía, Universidad Nacional Autónoma de México,*
Av. Xochicalco S/N, Temixco, Morelos, 62580, México,
Tel: +52-55-56229747, Fax: +52-55-56229742.
[b]*Centro de Física Aplicada y Tecnología Avanzada, Universidad Nacional Autónoma de México,*
Blvd. Juriquilla No. 3001 Juriquilla, Qro. 76230, México,
Tel: +52-44-22381173 Ext. 132,
e-mail: mcaa@fata.unam.mx, hzh@cie.unam.mx,
antonio@servidor.unam.mx, ohsa@cie.unam.mx .

Recibido el 14 de marzo de 2008; aceptado el 18 de septiembre de 2008

In this paper we present a systematic study into the influenc of the electrical, structural and optical properties of the porous silicon (PS) layers on the photovoltage and J –V responses of devices prepared from this semiconductor material. Electronic devices were prepared forming a p- or n-type PS (pPS and nPS, respectively) layer on crystalline silicon c-Si (p- or n-type, pSi and nSi, respectively) substrate. Two different metals were deposited as contact electrodes. The devices' electrical responses analyzed were their current density versus voltage (J-V) and photovoltaic. It was found that the presence of the pPS layer significantl modifie the electrical responses mentioned above of the pSi material. It means the optoelectronics properties of the pSi are modifie by the presence of the pPS layer; it can be understood in terms of the optical absorption spectra of PS. The nPS does not modify the optoelectronic properties of the nSi material. We propose an energy band diagram in order to explain the different behavior of these two different PS layers.

Keywords: Porous silicon; photovoltage; electrical properties.

En este artículo presentamos un estudio sistemático acerca de la influenci que tienen las propiedades eléctricas, de estructura y ópticas del silicio poroso (PS) sobre las respuestas de foto-voltaje y J-V de los dispositivos preparados con este material. Dispositivos electrónicos son preparados formando una capa de PS (tipo p o tipo n, pPS y nPS respectivamente) sobre un substrato de silicio cristalino (tipo p o tipo n, pSi y nSi respectivamente). Dos metales diferentes son depositados como electrodos de contacto. Las respuestas eléctricas de densidad de corriente contra voltaje (J-V) y fotovoltaica son analizadas. Se encontró que la presencia de la capa pPS modific significat vamente las respuestas eléctricas, mencionadas anteriormente, del material pSi. Esto signific que las propiedades optoelectrónicas del pSi son modificada por la presencia de la capa de pPS, lo cual puede ser entendido en términos del espectro de absorción óptica del PS. La película de nPS no modific las propiedades optoelectrónicas del material nSi. Proponemos un diagrama de bandas de energía para explicar este comportamiento diferente de las capas de PS.

Descriptores: Silicio poroso; fotovoltaje; propiedades eléctricas.

PACS: 73.40.-c; 73.40.Ei; 73.40.Lq; 85.60.-q; 85.60.Bt

1. Introduction

It is well known that a porous silicon (PS) layer can be formed on one side of a crystalline silicon wafer (c-Si) by an electrochemical etching process, the PS layer, which looks like a sponge with a rigid silicon skeleton and columnar open pores. The morphology of the PS layers depends on the c-Si conductivity type and etching conditions basically. It has been shown that the p-type PS (pPS) layer has distributed micro- and nano pores (so named because of the pore size), whereas an n-type PS (nPS) usually contains macropores and has a rough surface [1]. Due to the small size of the silicon structures in the PS layers, the quantum effect [2] is observed: the forbidden band-gap (Eg) energy value of a PS layer is greater than that of the c-Si, in spite of the discrepancies in the classificatio according to whether the PS electronic transition are indirect [3,4] or direct [5].

On the other hand, a few studies on PS for photovoltaic application have been reported. For example, at the beginning of the nineties a photovoltaic device based on pPS/pSi was prepared, showing an open circuit voltage ($V_{OC)}$ about 365mV and a short circuit current density (J_{SC}) on the order of μA [6]. It has been shown that the V_{OC} level depends on the excitation light power [7,8], annealing process and exposure time to different aging ambients [9]. The J_{SC} behavior in self-supporting PS sandwiched between ITO was studied by transient photoconductivity [10]. However, a systematic study on the relations between the photovoltage and J-V characteristic of the PS based photovoltaic device and the optical absorption coefficien of the PS layer has not yet been determined. It represents the main objective of this work.

2. Experimental

Devices were prepared on (Phosphorous doped) and p (Boron doped) c-Si wafer (Czochralski, Atomergic Chemetals Corp.), with (100) orientation and 10 Ohms-cm resistivity. Wafers were cleaned with a HF/ethanol solution for about 3-5min prior to the formation of the PS layer. The PS lay-

ers were formed by an electrochemical process, using a 1:1 HF (48%wt)/ethanol (98%wt) solution inside of a Teflo cell, and a current power supply. The applied current density was 20 mA/cm^2 for 35 seconds to form a PS layer less than 1 μm thick. In the case of nSi, the front side was exposed to the illumination of a 50-watt lamp at a distance of 10 cm from the cell during the etching process. This is necessary in order to form the PS layer because of the lack of holes in the nSi substrate [1]. PS samples were rinsed and kept in ethanol for about 5 min, and then dried with N_2 gas.

The estimate of the porosity and thickness of the PS layers was made by gravimetric measurement and Scanning Electron Microscopy (SEM), respectively. Thickness and porosity of the PS layers were about 640 nm and 73% for pPS prepared from the pSi substrate (Fig. 1) and around 774 nm and 56% for nPS prepared from the nSi, respectively. Current-Voltage (J-V) curves were obtained using a current-voltage source Keithley 230. Photovoltage spectra (zero current) were obtained using a Corner Stone 1/8m Oriel monochromator. Both J-V and photovoltage responses results were obtained from average measurements of at least four samples. Optical absorption spectra of free-standing pPS layers were recorded on a Shimadzu spectrophotometer UV3101 PC. The glancing incidence X-ray diffraction of PS was carried out at incident beam angles (Ω) of 0.3-2.0°, in a Rigaku DMAX-2200 X-ray diffractometer with Cu Kα radiation to verify the crystallinity.

To study the influenc of the PS layer on the electrical performance of c-Si photovoltaic devices it is necessary to prepare the corresponding devices firs without the PS layers. A metal1/c-Si/metal2 device was prepared by evaporating Aluminum (Al) on the back side of c-Si as metal2 and with the physical contact copper (Cu) wire on top of a c-Si wafer as metal1.

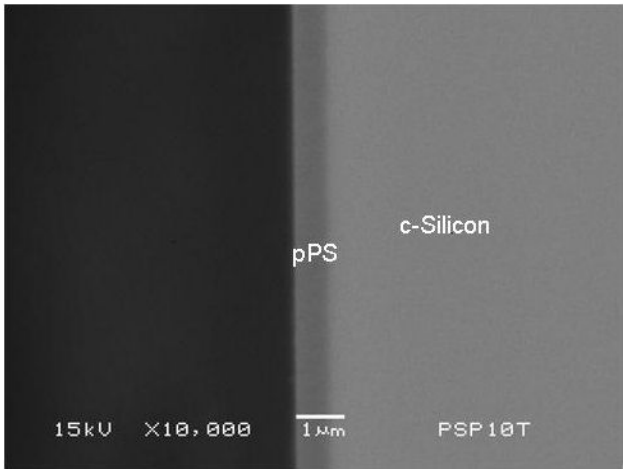

FIGURE 1. SEM image of the cross section of the pPS on p-crystalline silicon substrate.

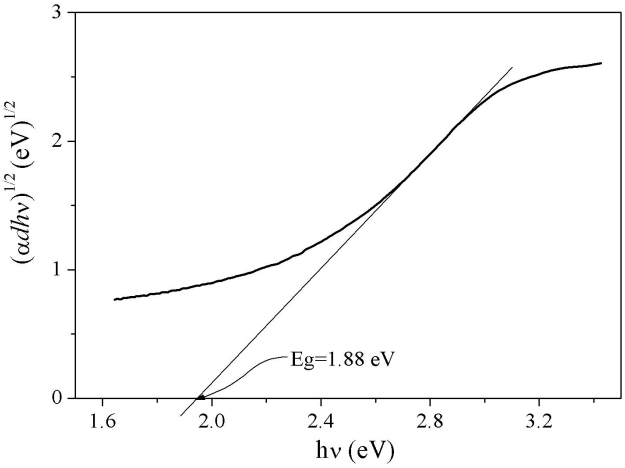

FIGURE 2. Absorption coefficien (α) as a function of photon energy (hν) for indirect electronic transitions in a free-standing pPS layer peeled off from its p-type silicon substrate.

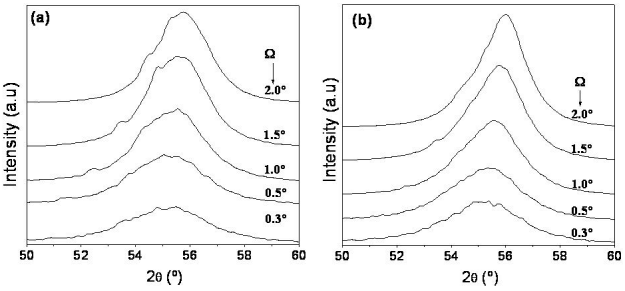

FIGURE 3. X-ray diffraction patterns at different incident beam angles (Ω) of porous silicon layers on (a) nSi and on (b) pSi substrates. The intensity of the peak is not normalized.

3. Results and discussion

Figure 2 shows the absorption coefficien (α) as a function of the photon energy ($h\nu$) for a free-standing thick pPS layer without its pSi substrate. The plot shows a linear dependence on $h\nu$, giving 1.88 eV for an indirect Eg [11]. This value is close to 1.7 eV for a pPS layer (74% of porosity) obtained from pSi (1 Ohms-cm) [3], and even closer to 1.8 eV, the value used to understand the electrical behavior in Light Emitting Devices (LED's) [12]. Therefore, the experimental Eg value of 1.88 eV for pPS layers will be used here to explain the photovoltaic behavior of PS based devices. It is not possible to perform this kind of characterization for nPS since this layer cannot be peeled off from the nSi substrate [1].

Diffraction patterns (Fig. 3) of the thick nPS (Fig. 3a) and pPS (Fig. 3b) layers on their respective c-Si wafers were taken at different incident beam angles (Ω) from 0.3 to 2.0°. Angle variation is used in order to get the response of the PS layer without the influenc of the c-Si substrate. The patterns of nPS and pPS show a broad diffraction peak located at $2\theta \sim 56^o$ for Ω = 2.0°, corresponding to (3 1 1) plane reflectio of c-Si at 56.5628, as reported elsewhere [13]. AFM images of the surface morphology of the nPS and pPS, respectively, on silicon substrate, are shown in Fig. 4.

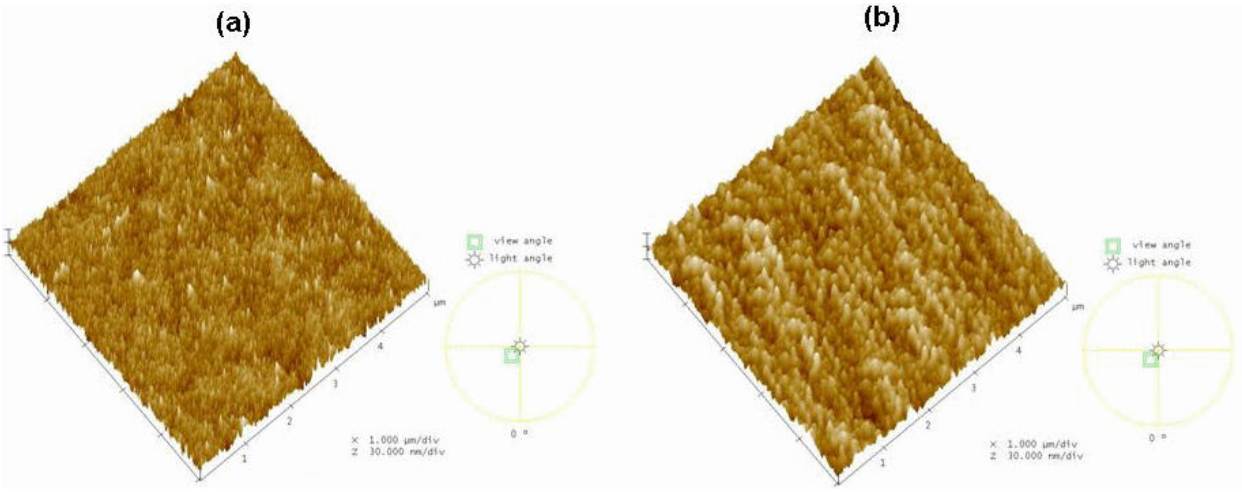

FIGURE 4. AFM images of (a) nPS and (b) pPS on a surface of 5μm. PS-1:1 HF/ethanol, 20mA/cm^2, $35s$.

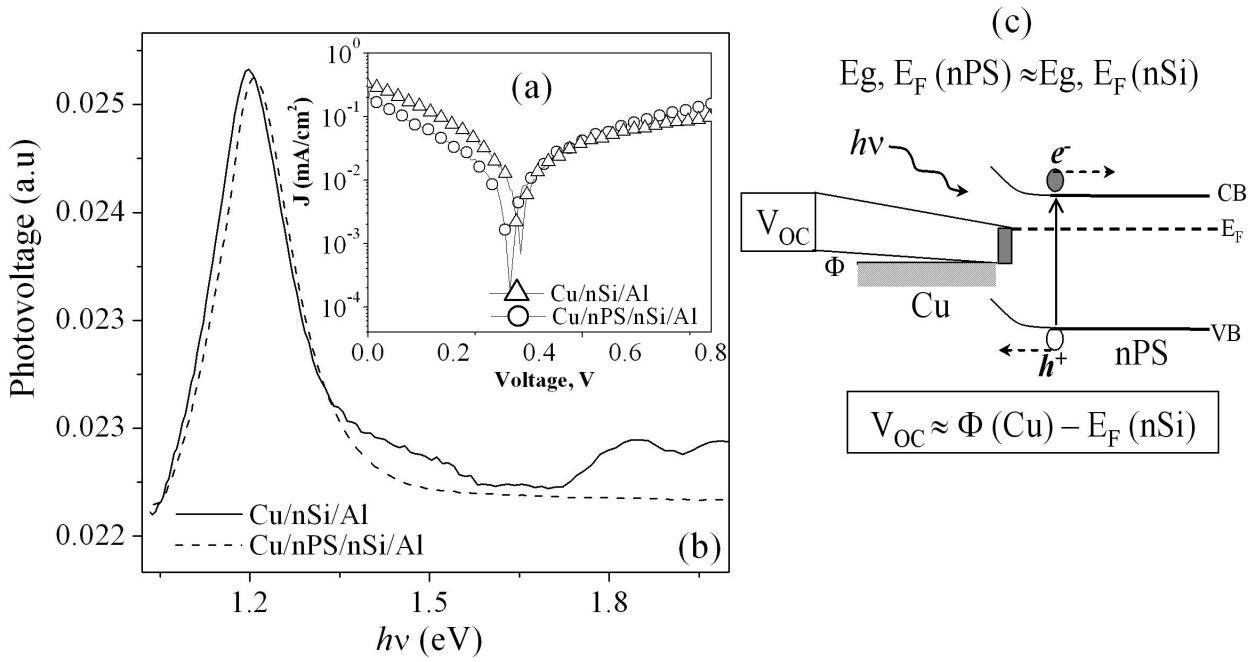

FIGURE 5. (a) Current-Voltage curves of (-) Cu/nSi/Al (+) (open up triangles) and (-) Cu/nPS/nSi/Al (+) (open circles) devices. (b) Photovoltage spectra of (-) Cu/nSi/Al (+) (solid line) and (-) Cu/nPS/nSi/Al (+) (dash line). (c) Scheme of the energy band diagram of the Cu/nSi junction.

Figure 5a shows the J-V curves under illumination from both the single nSi wafer and nPS/nSi junction; the positive bias was applied on the Al side from -1 to 1V. The illumination on the device is made through the PS or cleaned c-Si front side with a power intensity of 59.4mW/cm^2. The dark J-V curves of these devices are not shown, because they presented similar characteristics with a low rectifying ratio (F_R= I_{max}/I_{min}) of about 20 at 1V. It is observed in Fig. 5a that the current density under illumination from the Cu/nSi/Al device is of almost the same order of magnitude as that of the Cu/nPS/nSi/Al. However the PS layer improves the rectifying behavior since the $F_R$value increases from 36 to 99. Both devices show the photovoltaic effect with similar V_{OC} and J_{SC} values: 355mV and 0.32mA/cm^2 for the Cu/nSi/Al device, and 330mV and 0.20mA/cm^2 for the Cu/nPS/nSi/Al device, respectively.

Figure 5b shows the behavior of the photovoltage curves as a function of the photon energy of the same devices in Fig. 5a. The broad peak from 1 to about 1.5 eV exhibits a maximum around 1.2 eV, which should be related to the c-Si optical band gap (1.12 eV). It is observed that the presence of an nPS layer on nSi wafer causes a slight shift in this maximum peak to a higher energy, but it does not generate a notable change in the devices' electrical properties, Fig.5a. This suggests that the nPS layers should have a very similar Eg value to that of the nSi substrate because the Si skeleton dimensions are too large to expect quantum size effects in this type of PS layers [2,5]. On the other hand, the thickness

of the nPS layer has no influenc on the photovoltage spectra of the devices; nPS layers 50 and 1 μm thick shows the same photovoltage spectrum response.

Base on the results presented above, an energy band diagram model can be built for the device in Fig. 5. According to the electrical properties and the energy band diagram, the Cu/nSi/Al device V_{OC} level shown, about 330 mV, could be related to the difference between the work function of the Cu ($\Phi \approx 4.6$ - 4.7) and the Fermi level of the nSi substrate ($E_F \approx 4.31$eV to 10 Ohms-cm [11]). The internal electric fiel ξ formed in the Cu/nSi interface allows the free electrons and holes generated to reach their respective metal contacts (Fig. 5c). The photovoltage spectrum of the nPS device is produced by the photogeneration of both electrons and holes in the nSi layer for photon energies greater than 1.12 eV.

On the other hand, Cu/pSi/Al and Cu/pPS/pSi/Al devices, behave quite differently. In dark conditions, when a pSi wafer is in contact with Cu and Al, a rectifie diode behavior is presented (not shown). The Cu/pPS/pSi/Al device shows the exponential behavior of the current for forward bias (pSi positive with respect to pPS) (Fig. 6a). Table 1 summarizes the two devices electrical parameters obtained from [11], where R_S is the serial resistance, R_{SHUNT} is the shunt resistance, Jo is the saturation current density, F_R is the rectifie ratio, n is the ideality factor, and $V_{OC}$and J_{SC}were described above. The F_R of the pPS diode is about 2×10^3 at 1V, one order of magnitude greater than that of the pSi device without pPS. The non-ideal behavior (n¿1) of the devices can be attributed to the recombination mechanism in the depletion region.

Under illumination (59.4 mW/cm^2 through PS side), the Cu/pSi/Al did not exhibit any significan photovoltaic effect (Table I). However, the Cu/pPS/pSi/Al device showed a V_{OC} and J_{SC} of 235 mV and 0.13 mA/cm^2 (Fig. 6a and Table I). The $F_R$is lower by two orders of magnitude (60 at 1V) than the dark conditions (2×10^3 at 1V) one. The fil factor (FF) of the pPS cell is about 0.3 calculated by: $FF = (V_{\max}J_{\max}/V_{oc}J_{sc})$. This value could be due to the high device resistances, which affect its performance. The conversion efficien y (n_c) is about 0.016%, calculated by the relation: $n_c = (V_{oc}J_{sc}FF/P_{in}) \times 100$, where P_{in} is the power intensity on the device measured with a pyrometer. It is important to mention that due to the chemical activity of the PS, the PS layer is not free of impurities, which can affect the conversion efficien y.

TABLE I. Electrical parameters of the pPS devices prepared on pSi substrate.

Device	J_O (mA/cm^2)	F_R at 1V (dark)	n (Potential interval)	R_S (Ohms)	R_{SHUNT} (Ohms)	V_{OC} (mV)	J_{SC} (mA/cm^2)
Cu/pSi/Al	0.17	1×10^2	2.03 (0.04-0.17V)	1239	——	——	——
Cu/pS/pSi/Al	1.59×10^4	2×10^3	1.89 (0.05-0.33V)	8557	5.8×10^5	235	0.13

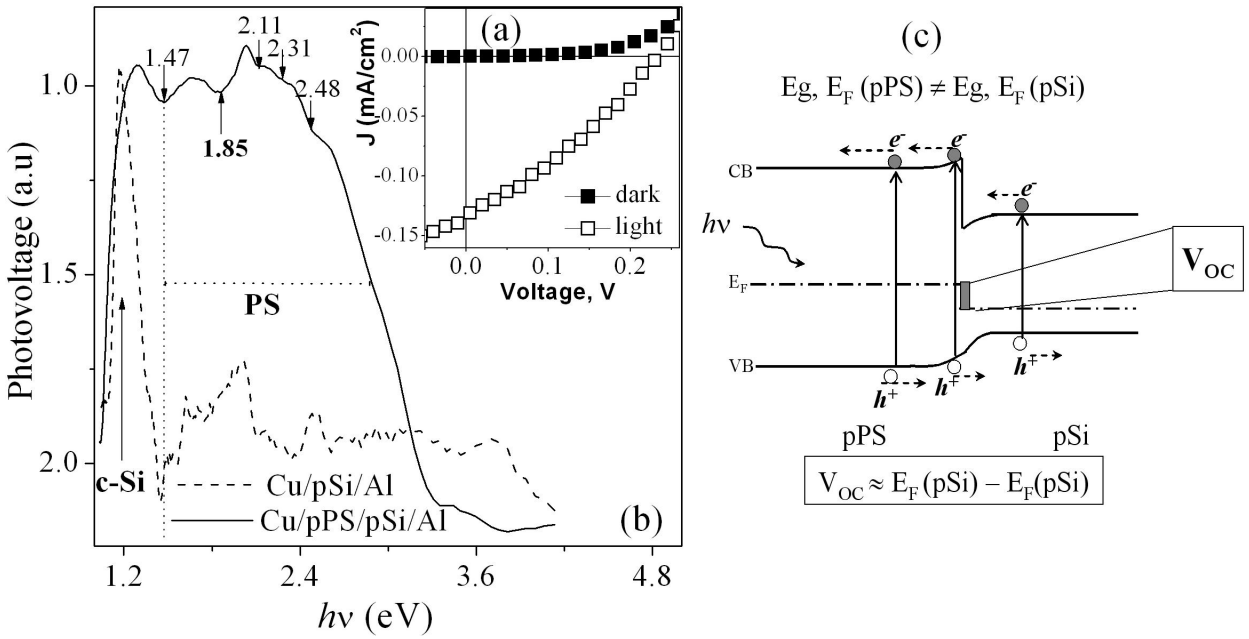

FIGURE 6. (a) J-V curves of Cu/pPS/pSi/Al device in dark (I) and under illumination (II). (b)Photovoltage response of Cu/pPS/pSi/Al device (solid line) compared with the photocurrent response of Cu/pSi/Al device (dash line) as a function of photon energy. (c) Scheme of the energy band diagram of the pPS/pSi junction.

Figure 6b shows the photovoltage response for the Cu/pPS/pSi/Al device. The photovoltage curve of the Cu/pSi/Al device is almost zero (not shown), which is in agreement with its J-V results. However, its photocurrent response is in the range of 1.2 to 1.5eV (Fig.6b dash line), similar to the photovoltage response of the nSi substrate. For the pPS/pSi device, the photovoltage shows a broad response starting from about 1eV and falling by up to 3.25eV, which can be separated into two zones: (1) the infrared region (1-1.47eV), and (2) the visible one (1.47 eV - 3.25 eV). The spectrum features in the firs region should be attributed to the contribution of the light absorption in the bulk c-Si substrate, according to the photocurrent response of the pSi substrate (Fig. 6b). The high energy part of the photovoltage curve should be related to the optical absorption in the PS layer, which starts at 1.47eV as has been reported [8]. A slight decrement at 1.85eV is also presented, which corresponds to the photoluminescence peak (1.84eV) of PS [14,15]. In addition, steps in the photovoltage spectra edge are observed in the energy range of 2.11-2.63eV [8], the average difference between the neighboring steps is correlated with the diameters of silicon wires and attributed to their discontinuous distribution in the porous silicon layer. The solid line spectrum in Fig. 6b shows only four steps and the average between them of 0.17eV $\pm$0.02eV indicates that the distribution of Si wires in this PS layer is quite homogeneous (see Fig. 6b).

From the experimental optical absorption data (Eg $\approx$1.8eV), the electronic affinit χ $\approx$3.6eV[12] of PS, the E_F $\approx$4.99eV for pSi of 10 Ohms-cm [11] and Eg of crystalline silicon of 1.12 eV, an energy band diagram for the Cu/pPS/pSi device can be built (Fig. 6c). After the junction formation, the internal electric fiel ξ formed in the pPS/pSi interface allows the opposite charge carriers to reach their respective metal contacts: electrons to Cu through PS and holes to Al through pSi. The photovoltage spectrum of the device is produced by the photogeneration of both electrons and holes in pSi for photon energies greater than 1.12 eV and in PS for more than 1.8eV. The V_{OC} value obtained in the J-V curves could be related to the difference in the Fermi level value on the PS/pSi interface in the following way: from the E_F $\approx$4.99eV for pSi of 10 Ohms-cm [11] and the experimental $V_{OC}$of 235 mV, it suggests that the E_F of pPS should take on a value of: E_F = 4.99-0.235 $\cong$ 4.75eV.

4. Conclusions

Porous silicon (PS) based on photovoltaic cells were fabricated by the electrochemical etching of both n- and p-type c-Si wafers with a (100) orientation and a resistivity of 10 Ω-cm. Although metal contact of n-type silicon (Cu/nSi/Al) gives an open circuit voltage of about 355 mV, the junction of nPS on nSi does not generate any photovoltaic current. The photovoltage response of the same device exhibits a very small shift in the maximum peak compared with that of the c-Si, suggesting that the nPS layers present the same Eg as c-Si. However, the PS layers obtained on the pSi show an indirect band gap of 1.88eV measured by optical absorption experiments, which is greater than that of crystalline silicon wafers (1.12eV). The photovoltage responses of the junction between the PS layers and pSi contain contributions from the two components of the junction: around 1.2 eV due to the c-Si and around 1.8 eV due to the PS layer. Metal contact of pSi does not show any photovoltaic effect, but a Cu/pPS/pSi/Al device gives an average value of 235 mV for Voc and 0.13 mA/cm^2 for J_{SC}, which comes from the pPS/pSi junction. The crystallinity of PS was shown by glancing incidence X-ray diffraction. According to the energy band diagrams of the two devices, the V_{OC} of n-type silicon comes from the energy difference between the metal contact and Fermi level of silicon, whereas in the case of the p-type device, it originates from the different Fermi level between the porous silicon layer and its crystalline wafer.

Acknowledgements

The authors wish to thank M.L. Ramón-García for XRD measurements, G. Casarrubias-Segura and J. Campos for electrical characterizations, A. del Real for SEM image and A.G Palestino-Escobedo for AFM images. Financial support from CONACyT (42794 and G38618) is acknowledged. MCA wishes to thank CONACyT and DGEP-UNAM for financia aid during her doctoral program.

∗ Corresponding author

1. M.C. Arenas, H. Hu, J.A. del Río, A. Sánchez, and M.E. Nicho, *Sol. Energy Mater. Sol. Cells* **90** (2006) 2413.
2. L.T Canhman, *Appl. Phys Lett.* **57** (1990) 1046.
3. I. Sagnes, A. Halimaoui, G. Vincen, and P.A. Badoz, *Appl. Phys Lett.* **62** (1993) 1155.
4. J.E. Lugo, J.A. del Río, and J Tagüeña-Martínez, *Sol. Energy Mater. Sol. Cells* **52** (1998) 239.
5. Z.-C. Feng and R. Tsu, *Porous Silicon*, World Scientific London, 1994.
6. G. Smestad, M. Kunst, and C. Vial, *Sol. Energy Mater. Sol. Cells* **26** (1992) 277.
7. Z. Han, J. Shi, H. Tao, Li Gong, Shaojun fu, Chaoshu Shi, and Xingyi Zhang, *Phys. Lett. A* **186** (1994) 265.
8. F. Yan, X-M Bao, and T. Gao, *Sol. State Communications* **91** (1994) 341.
9. P.K. Kashkarov, E.A. Konstantinova, A.B. Matveeva, and V. Yu. Timoshenko, *Appl. Phys A* **62** (1996) 547.
10. R. Sedlaèik, F. Karel, J. Oswald, A. Fejfar, I. Pelant, and J. Koèka, *Thin Solid Films* **255** (1995) 269.

11. S.M. Sze, *Physics of Semiconductor Devices*. John Wiley and Sons, New York, 1981.

12. C. Peng, K.D. Hirschman, and P.M. Fauchet, *J. Appl. Phys.* **80** (1996) 295.

13. M. Banerjee, E. Bontempi, A.K. Tyagi, S. Basu, and H. Saha, *Applied Surface Science* **254** (2008) 1837.

14. X. Wang *et al.*, *Phys. Rev. Lett.* **71** (1993) 1265.

15. S.L. Zhang *et al.*, *Appl. Phys. Lett.* **62** (1993) 642.